K. C. Pandey

Reaction of Atomic Hydrogen with Si(111) Surfaces: Formation of Monohydride and Trihydride Phases

Abstract: By using a realistic tight-binding or LCAO (linear combination of atomic orbitals) model, detailed calculations of surface states, local densities of states, and theoretically simulated photoemission spectra have been carried out for two qualitatively distinct structural models for chemisorption of atomic hydrogen on Si(111)1×1 surfaces. In the low-coverage model, called the monohydride phase or Si(111):H, it is assumed that a single hydrogen atom sits on top of each surface Si atom, thus saturating all dangling bonds. In the high-coverage model, designated as the trihydride phase or Si(111):SiH_3, SiH_3 radicals are bonded to the surface Si atoms. Due to the radically different atomic structures, the theoretical spectra of the two phases show striking differences. A comparison of the theoretical spectra with the ultraviolet photoemission spectra taken during hydrogen chemisorption on the quenched Si(111)1×1 surface clearly shows that at low coverages the monohydride is formed, while at high coverages the trihydride phase is formed. Formation of the monohydride phase is expected on simple chemical and structural considerations, and it has been observed on other Si surfaces. However, formation of the trihydride phase is unique to Si(111)1×1 and as such, it has important implications regarding the structure and stability of clean Si(111)1×1.

Introduction

Of all the semiconductor surfaces, the electronic structure of the Si(111) surface has been studied most extensively, both experimentally [1–3] and theoretically [4–7]. It is well known, from LEED (low energy electron diffraction) studies, that the atomic structure of this surface, like those of most other semiconductors, differs from that of an ideal truncated lattice [8, 9]. In the terminology of surface crystallography, the surface is "reconstructed." In fact, depending on the mode of preparation, three different phases of reconstruction may be obtained for the clean Si(111) surface: 1) the vacuum-cleaved metastable 2×1 surface [8, 9]; 2) the annealed 7×7 surface [8, 9] which, near room temperature, is the thermodynamically most stable phase; and 3) the 1×1 phase [10], stable only at temperatures higher than ≈1300 K. However, the 1×1 surface can be stabilized at room temperature by rapid cooling [10] to give a metastable "quenched 1×1" phase [11].

Ultraviolet photoemission spectroscopy (UPS) has been used by several workers [1–3] to study the surface electronic states of Si(111) surfaces. Angle-integrated UPS spectra at a photon energy of ≈20 eV essentially reflect a weighted average of the occupied surface states and the states of the underlying bulk solid in the outer few layers. For all three phases the UPS spectra at $h\nu$ = 21.2 eV show three dominant peaks [1–3]: a large, broad peak at $(E - E_{vac}) \approx -8.0$ eV, a narrower peak at $(E - E_{vac}) \approx -12.0$ eV, and a small peak at $(E - E_{vac}) \approx -15.0$ eV, where E_{vac} is the energy of the vacuum level. These structures, which do not depend on the reconstruction phase, are obviously due to the bulk energy bands of the underlying crystal, and are well understood. Surface effects are reflected in the UPS spectra as a number of less pronounced structures superimposed on these three peaked spectra. Several of the observed surface features have been attributed [4–7] to the surface states arising from the broken bonds (dangling orbitals) at the surface, the rehybridization of these dangling orbitals due to the relaxation or atomic rearrangement at the surface, and the resulting modifications of backbonds.

The UPS spectra of all three Si(111) surfaces change drastically on exposure to atomic hydrogen [3, 10, 12, 13]. Figure 1 shows the angle-averaged UPS spectra [10] at a photon energy of 21.2 eV for the clean and H-covered quenched Si(111)1×1 surfaces. At low H coverages, two well-defined H-induced peaks develop at $(E - E_{vac}) \approx -10$ and -12 eV. On increasing H exposures, these peaks grow in intensity until an intermediate H-saturated spectrum, shown by the middle curve in Fig. 1, is obtained (the H-induced peaks are denoted by C and D). For reasons to be discussed later, we will refer to this spectrum as the monohydride or

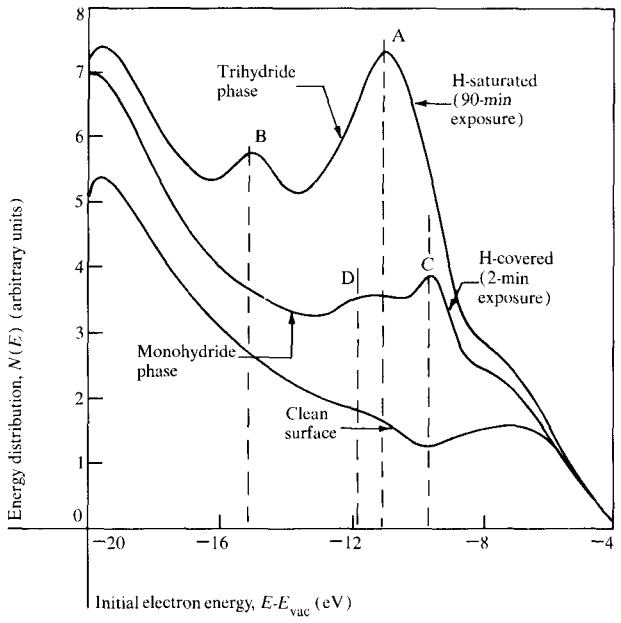

Figure 1 Ultraviolet photoemission spectra of clean and hydrogen-covered Si(111)1×1 surfaces at a photon energy of 21.2 eV. Theoretical analysis of these spectra shows that the low-coverage spectrum is due to the monohydride phase, Si(111):H, while the high-coverage spectrum is due to the trihydride phase, Si(111):SiH_3.

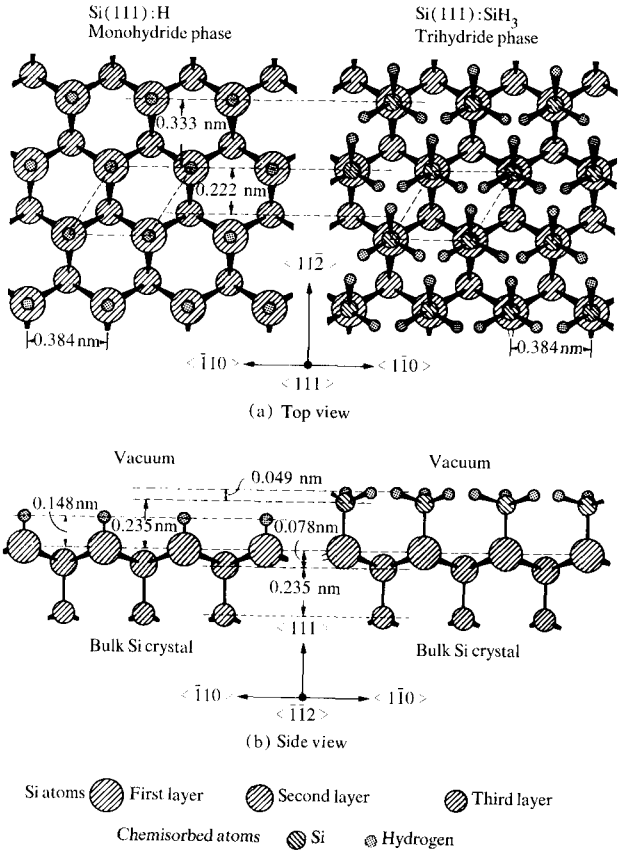

Figure 2 Atomic structural models for the monohydride and trihydride phases of the Si(111)1×1 surface saturated with hydrogen. The Si–H bond length, in both phases, is assumed to be 0.201 nm. All Si atoms are assumed to be in their ideal bulk position.

Si(111):H spectrum. The UPS spectra of both the cleaved and the annealed surfaces also undergo similar changes on H exposure, giving H-saturated spectra that are very similar to the monohydride spectrum, both in the peak positions and in their relative heights. While the spectra of the cleaved and annealed surfaces do not change on further H exposure, two new peaks, at $(E - E_{vac}) \approx -11$ and -15 eV, develop on the 1×1 surface. The high-coverage saturation spectrum is shown by the top curve in Fig. 1, and we will refer to it as the trihydride or Si(111):SiH_3 spectrum. It is clear that the two H-saturated spectra (low and high coverage) are quite distinct, differing not only in the heights of the H-induced peaks but also in their energies. Larger peak heights in the trihydride phase, as compared with the monohydride, are a clear indication of a larger H coverage in the former. This is further supported by a much larger H uptake [10] in the formation of the trihydride phase. As indicated by the changes in the energies of the H-induced peaks, the nature of the bonding of H atoms to the Si(111) surface is also quite different in the two phases. These changes in the peak positions and their heights strongly suggest that there are two distinct structural phases for H chemisorption on the quenched surface.

In order to understand these changes in the electronic structure of the Si(111) surface caused by chemisorbed hydrogen and, in particular, to determine the surface atomic structures [14] responsible for them, we have carried out detailed theoretical calculations of surface electronic states for several structural models for H chemisorption on the Si(111)1×1 surface. In this paper we discuss the calculations for two basic structural models that explain the UPS spectra for low and high coverages, respectively. These models are schematically shown in Fig. 2. In the monohydride or Si(111):H phase, shown in the left panel, a single hydrogen atom sits on top of each Si atom of the ideal Si(111)1×1 surface to form a normal Si-H covalent bond, thus saturating all dangling bonds. Considering the structure of the ideal Si(111) surface, in which each surface atom has one dangling orbital pointing perpendicular to the surface, this is on chemical grounds [15] the simplest and most plausible model. This model assumes a perfect 1×1 periodicity and, strictly speaking, can be applied only to the quenched and cleaved surfaces, which, on saturation

coverage, show the ideal 1×1 LEED structure, but not to the annealed surface, which transforms to a 7×1 structure after saturation coverage of H. We find, however, that the central assumption of the model (that covalent bonds are formed at the surface) is essentially true of the cleaved, the annealed, and the low-coverage quenched 1×1 surfaces. The structural differences between the hydrogen-saturated 7×1 and 1×1 surfaces are probably due only to differences in long-range ordering. The local ordering, i.e., the formation of a single Si–H bond with each surface atom, is the same in all three cases. In the assumed trihydride phase, shown in the right panel of Fig. 2, a single SiH_3 radical makes a covalent Si–Si bond with each surface Si atom. The trihydride structure can also be obtained by removing an entire layer of Si atoms from the clean ideal surface and saturating each of the three dangling bonds on the second-layer Si atoms with hydrogen atoms. The Si–H bond length, in both phases, is assumed to be 0.201 nm, the same as in the SiH_4 molecule [16]. All Si atoms are assumed to be in their ideal bulk position.

By using a self-consistent pseudopotential method, a theoretical study of the chemisorption of atomic hydrogen on the ideal Si(111) surface has recently been carried out [17]. However, this calculation was limited only to the monohydride phase and no detailed comparison with experimental data was made. In the present paper, calculations for both the monohydride and the trihydride phases are presented, and from a detailed comparison with UPS spectra we show that, in addition to the previously studied monohydride phase, the perhaps unexpected trihydride phase also exists. In contrast to the previously used pseudopotential method, we take a computationally much simpler but physically more transparent tight-binding approach. Such an approach is attractive because of its immediate connection with ideas on chemical bonding. While in the past we have demonstrated the usefulness of the tight-binding method in surface studies [5–7], these studies were limited to clean surfaces, e.g., the ideal and relaxed (111) and (100) surfaces of Si and Ge. One of the motivations for this study was to determine whether the tight-binding approach could be extended to chemisorption studies as well. For the monohydride phase, we find good quantitative agreement between the present calculation and those based on the *ab initio* method [17], confirming the validity of our tight-binding model for chemisorption. The simplicity of our method allows us to carry out, for several possible structural models, a very detailed calculation of the surface energy bands, local densities of states, and simulated photoemission spectra that can be directly compared with the UPS spectra. This allows us to identify the new trihydride phase. Because of the localized orbital representation used in the tight-binding model, simple molecular symmetry orbital assignments can be made to surface states.

In this paper, we discuss the tight-binding model and the determination of the Hamiltonian matrix elements between different atomic orbitals. We also give a brief description of the calculations of the surface states and local densities of states. The results are discussed and a comparison with experimental spectra is made. A brief discussion of the nature and origin of various surface states and associated peaks in the UPS spectra is also given.

The tight-binding model for chemisorption

The semi-empirical tight-binding model used to study the chemisorption of hydrogen is based on the concept of 'bond transferability,' and has been discussed in detail elsewhere [12, 15]. The basic assumption underlying this model, which is based on the Hückel approximation (i.e., the orthogonalized atomic orbitals form the basis functions), is that the chemisorption bond between the substrate atoms and the adsorbate is very similar to the corresponding bond in an appropriately chosen molecule. Thus, for example, for the study of chemisorption of hydrogen on the Si(111) surface we assume that the Si-H bond length at the surface and in SiH_4 are the same. The assumption of bond transferability not only means that the bond lengths remain unchanged in going from one system to the other, e.g., from a molecule to the surface, but it also implies that the bonds are similar in every respect and that all the physical parameters used to describe them can be assumed to remain essentially unaltered. To be more specific, the orthogonalized orbitals describing the bond, the potential in the internuclear or bond region, and hence the Hamiltonian matrix elements, remain the same.

There is an overwhelming amount of chemical data [15] supporting the concept of bond transferability. It is a well-known fact [15, 17] that the bond lengths and energies between a pair of atoms remain essentially the same, even in quite diverse systems where the long-range (and even the next-neighbor) atomic arrangements and bonding may be drastically different. For example [17], within the limits of experimental accuracies, Si–Si bond lengths and dissociation energies in Si_2H_6 and crystalline Si are identical; the same is true of Si–H bonds in Si_2H_6 and SiH_4.

An ingredient essential to the tight-binding calculation [6, 12, 18, 19] is the knowledge of the Hamiltonian matrix elements or interaction parameters between the various atomic orbitals involved. While a first-principles calculation [18] of these matrix elements is possible, and is routinely performed in most of the first-principles molecular calculations involving first-row atoms, in this paper we take a simpler semi-empirical approach. In semi-empirical tight-binding (SETB) methods [6, 12] the interaction parameters are obtained from the electronic states of a molecule or solid that contains the bond in question and

whose electronic states are known either from experiments or from *ab initio* calculations. In order to calculate the surface states associated with hydrogen chemisorption on Si(111) (for which structural models are shown schematically in Fig. 2), we need to know the parameters associated with the interaction of Si-Si, Si-H, and H-H orbitals.

The tight-binding method used in the present paper has been described in detail elsewhere [6, 12]. To summarize briefly, we use the minimal basis set; i.e., only one s and three p orbitals of the valence shell of each Si atom and one 1s orbital of each H atom are included in the basis set. As mentioned before, we assume that the atomic orbitals are orthogonalized. We also use the two-center approximation [19] and assume that all matrix elements between orbitals centered on atoms farther than the next nearest neighbors are negligible.

A detailed discussion of the determination of Si-Si matrix elements by least-squares fitting to the well-known bulk energy bands of Si at a large number of **k** points (wave vectors) in the Brillouin zone has been given elsewhere [6]. Because of the inability of the tight-binding model to represent conduction band states accurately, only the four valence bands and the lowest conduction band were included in the fitting procedure. The seven parameters [6] obtained from such a fitting procedure describe the bulk valence bands of Si over the entire Brillouin zone to an accuracy of about 0.2 eV. Of the seven parameters, one is the difference in the diagonal matrix elements or the atomic energy levels of p and s orbitals ($E_p - E_s$), four (ssσ, spσ, ppσ, and ppπ) are the matrix elements between the nearest-neighbor orbitals, and only two matrix elements, those involving p orbitals alone (ppσ and ppπ), represent the interaction between second-nearest-neighbor Si atoms. These seven matrix elements completely specify the interactions among Si orbitals.

Since the structural model (Fig. 2) assumed for hydrogen chemisorption does not involve any atomic displacement of the underlying Si layer, the electronic states of the ideal Si substrate (ignoring the hydrogen overlayer) are completely specified by the interaction parameters determined from the bulk [5, 6]. However, in order to study hydrogen chemisorption, we still need the matrix elements describing the interaction between the orbitals of H and the nearest-neighbor Si atom and possibly the matrix elements between the nearest-neighbor H-H orbitals as well. Assuming the validity of the concept of bond transferability, we take the Si-H bond length at the surface to be the same as that in the SiH_4 molecule. We also assume that two-center Hamiltonian matrix elements between the orthogonalized orbitals of Si and H for the two systems are the same. As in the SETB method, we determine the matrix elements between H and underlying nearest-neighbor Si orbitals from the experimentally known ionization potentials and electron affinities of SiH_4. This is the crucial assumption of the present calculation and can be taken as a more precise statement of our chemisorption model.

In order to relate the ionization potentials to the molecular orbital energy levels, which are the quantities calculated in the simple one-electron molecular orbital theory, we must assume the validity of Koopmans' theorem [20]. According to this approximation, the individual vertical ionization potentials may be equated with a negative sign to the one-electron energy eigenvalues of the molecular orbitals that are ionized. In most cases Koopmans' theorem holds only approximately [21]. However, the relative ionization potentials of various orbitals from the same molecule are affected much less by violation of Koopmans' theorem than are their absolute values. Thus, in order to minimize the errors in the parameters arising from violation of Koopmans' theorem, only the relative values of the various ionization potentials were used in our least-squares fitting procedure [10, 12].

Because of the tetrahedral symmetry of the SiH_4 molecule, there are only two distinct valence levels, a triply-degenerate molecular level of t_2 symmetry and a non-degenerate level of a_1 symmetry. The ionization potentials of these levels, as measured from the photoelectron spectra [22, 23] and listed in Table 1, are not enough to uniquely determine the three Si-H interaction parameters (the diagonal matrix element for hydrogen E_H, and the two matrix elements ssσ and spσ between the s and p orbitals of Si and the s orbital of the nearest-neighbor hydrogen atom). However, a first-principles calculation of the lowest two excited states of the SiH_4 molecule has been carried out [24], and these energies are also listed in Table 1. By using the energy levels of the excited states together with the measured ionization potentials, all three Si-H parameters can be uniquely determined via least-squares fitting. Detailed discussions of the molecular calculation and the fitting procedure can be found in [12].

Some of the lowest ionization potentials of Si_2H_6, derived from the photoemission spectra [23], are also listed in Table 1. These are labeled according to the symmetry of the corresponding molecular orbital [25]. Using the Si-H parameters derived from the molecular levels of SiH_4, we have also calculated the molecular levels of Si_2H_6. The Si-Si parameters (needed for the calculation of the molecular orbitals of Si_2H_6) were assumed to be the same as in the bulk Si crystal. The calculated molecular levels of both SiH_4 and Si_2H_6 are also listed in Table 1. As mentioned earlier, only the relative values of the ionization potentials were fitted. In order to make a comparison with the experimental data, we have adjusted the theoretical ionization potentials so that the lowest ionization potentials are approximately the same. As can be seen from Table 1, a reasonably good agreement with the ionization

Table 1 Ionization potentials for SiH_4 and Si_2H_6 molecules.

Molecule	*Orbital symmetry*	*Orbital energy levels* (eV)	
		Experimental	*Theoretical*[a]
SiH_4	a_1	−4.10 [24]	−4.01
	t_2	−5.40 [24]	−5.33
	t_2	−12.70 [22]	−12.62
	a_1	−18.20 [23]	−18.33
Si_2H_6	a_g	−10.70 [23]	−10.79
	e_g	−12.10 [23]	−12.50
	e_u	−13.30 [23]	−12.76
	a_u	−17.30 [23]	−16.91

[a]Theoretical ionization potentials refer to simple one-electron molecular orbital calculations.

Table 2 Interaction parameters (matrix elements) between a hydrogen s orbital and the s and p valence orbitals on the nearest-neighbor Si atom.

Parameters[a]	*Interaction parameters*[b] *for Si–H* (eV)
E_H	−3.38
$ss\sigma$	−3.57
$sp\sigma$	−2.76

[a]In the present calculation, these are obtained by fitting to the ionization potentials of SiH_4.
[b]Zero of energy was taken at the top of the bulk valence band of Si.

Table 3 The tight-binding interaction parameters (Hamiltonian matrix elements) for Si. (Note the systematic variation of the parameters.)

Parameters[a]	*Si–Si* (eV)[b]
$E_p - E_s$	4.39
$(ss\sigma)_1$	−2.08
$(sp\sigma)_1$	−2.12
$(pp\sigma)_1$	−2.32
$(pp\pi)_1$	−0.52
$(pp\sigma)_2$	−0.58
$(pp\pi)_2$	−0.10

[a]Subscripts 1 and 2 refer to the first and second nearest neighbors.
[b]Matrix elements were determined by the least-squares fitting of the bulk energy bands of Si at a large number of wave vectors.

potentials is obtained for both SiH_4 and Si_2H_6, even though the ionization potentials of the latter were not used in the fitting procedure. This serves as a check on our assumption of bond transferability, and demonstrates the reliability and accuracy of the Si-H interaction parameters that we have obtained.

The interaction parameters between the s orbital of H and the s and p orbitals of the nearest-neighbor Si atom to which it is directly bonded are listed in Table 2. Because of the small radial extent of the H 1s orbital, we assume that the Si-H interaction parameters between the orbitals farther than the nearest neighbors are negligible. The Si-Si interaction parameters [8, 9], which were determined independently from the bulk energy bands of Si, are listed in Table 3 for completeness. This latter set of parameters has been taken directly from our earlier calculations; no further adjustments have been made. These matrix elements are also used in the calculation of surface state energy bands and local densities of states. For the surface calculations the Si-Si interaction parameters are needed to describe the substrate. The parameters listed in Table 3 show the expected chemical trends; the second-nearest-neighbor parameters (denoted by subscript 2) are considerably smaller than those for the nearest neighbor (subscript 1). Also, the $pp\sigma$ matrix element is much larger than the $pp\pi$ matrix element. With the determination of these interaction parameters, all the Hamiltonian matrix elements are completely specified, and the eigenstates can be obtained in a straightforward way by matrix diagonalization.

Surface calculations and results

In the tight-binding approximation, surface states and resonances are most easily obtained by calculating the electronic states of a slab of finite thickness [6, 12, 26]. If the slab is sufficiently thick, its electronic states will be identical to those of a semi-infinite solid, except for the two-fold degeneracy arising from the two identical surfaces of the slab. For maximum speed of computation, one uses a slab of minimum thickness that still represents the semi-infinite solid with sufficient accuracy. Along the surface, the slab extends to infinity and the surface periodicity [6, 12, 26] is exploited through the two-dimensional Bloch theorem. In the present calculations, the slab consists of 28 atomic layers of Si for the monohydride and 26 layers of Si for the trihydride phase. These slabs are bounded on each side by the H layer. The position of the hydrogen layer relative to the underlying Si slab for both the monohydride and the trihydride phases is shown schematically in Fig. 2. With four orbitals for each Si atom and one for each H atom, the dimension of the Hamiltonian matrix that must be diagonalized for each surface wave vector $\mathbf{k}_s$ is $(2\times1) + (4\times28)$ or 114 for the monohydride, and $(2\times3) + (4\times26)$ or 110 for the trihydride phase. All results (surface energy bands, local densities of states in the middle of the slab, etc.) were checked as a function of slab thickness and the present slab thickness was judged to be adequate [12].

We calculated the local densities of states [6, 12] for different atomic layers by numerical integration using a

sample of 45 nonequivalent $\mathbf{k}_s$ points in the irreducible section ($^1/_{12}$) of the two-dimensional hexagonal surface Brillouin zone. By using a Fourier expansion [12] this basic sample of 45 points was augmented by a factor of 100 through interpolation. The method for obtaining the surface energy bands and local densities of states has been described in greater detail elsewhere [6, 12].

For both chemisorption phases, Fig. 3 shows the local densities of states [6, 12] at the surface hydrogen layer and the underlying Si layer to which it is bonded. Unlike the clean Si(111) surface [6], which has a half-filled surface state band near the top of the valence band, the hydrogen-covered Si(111) surfaces do not have any surface states in the gap. This is expected because the singly-occupied dangling orbitals (that give rise to these gap states), on making covalent bonds with hydrogen, are transferred into bonding orbitals, and lead to surface states at lower energies. Note that as a result of the removal of the dangling bond states near the top of the valence band, the Fermi energy E_F is no longer pinned.

It is evident from Fig. 3 that there are very significant differences between the local densities of states at the hydrogen layer for the monohydride and trihydride phases. If finer details are ignored, the monohydride spectrum is dominated by a single peak, while the trihydride phase shows two peaks. It is possible to understand these qualitative differences from simple arguments based on the symmetry of the sites of the surface Si and H atoms. In the monohydride phase, because the hydrogen atom sits on top of the underlying Si atom, there is only one bonding state (of σ symmetry) arising from the bonding of the hydrogen s and the sp_3 dangling orbital of the surface Si atom. For the trihydride phase, because of the threefold rotational symmetry about the surface Si atom, there are three possible bonding states, a nondegenerate state of σ symmetry and a doubly degenerate state of π symmetry. Because of the presence of the neighboring atoms, these molecular orbitals broaden into bands giving rise to rather wide peaks in the local densities of states. Peaks A and B (Fig. 1) in the trihydride spectrum arise from the π and σ states, respectively.

As a result of the covalent bond formation, the local density of states of the surface Si layer (Fig. 3) clearly reflects all the features of the H layer with which it is bonded. Thus, in Fig. 3, structures (C for the monohydride and A_1, A_2, B_1, B_2, and B_3 for the trihydride phase) in the local densities of states at the Si layer occur at the same energy and have the same lineshape as the corresponding structures in the H-layer local densities of states. However, there are additional structures in the local densities of states for the Si layer. These arise from electrons participating in the Si–Si backbonds and can be seen more clearly (F and G in Fig. 3) in the monohydride phase, where three of the four electrons contribute to

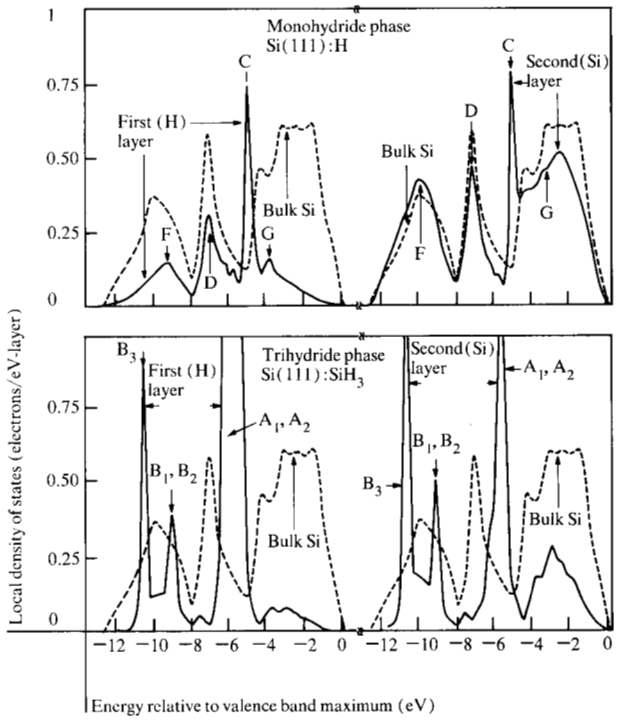

Figure 3 Local densities of states (solid lines) at the surface hydrogen layer and the first Si layer for the monohydride phase (top panel) are compared with the corresponding spectra for the trihydride phase (lower panel). The bulk density of states (dashed line) is also shown for comparison.

these states. These additional structures are weaker in the trihydride phase because only one of the electrons participates in the backbonding. As expected, their energy distribution is roughly similar to that for the bulk Si.

In addition to these bonding states, there is an empty state (not shown in Fig. 3) of σ antibonding character. This state is localized primarily on the underlying Si atom and is made up of its p_z (z axis is along the surface normal) orbitals, which give rise to the dangling-bond surface state on clean Si(111). On chemical grounds, localization of the empty states primarily on Si is expected, because H is more electronegative and there is appreciable electron transfer from Si to H. This empty surface state, which has not been previously predicted, should be observed in electron energy loss spectroscopy.

The strong spatial localization of surface states is clearly evident from the variation of the local densities of states at successive Si layers as we move down into the bulk crystal. The local densities of states rapidly approach the bulk value. Even at the fourth layer (not shown in Fig. 3), the local density of states differs from the bulk by only a very small amount, and at the middle of the slab it is almost identical to the bulk. In fact, this is one of the criteria used to test the convergence of our

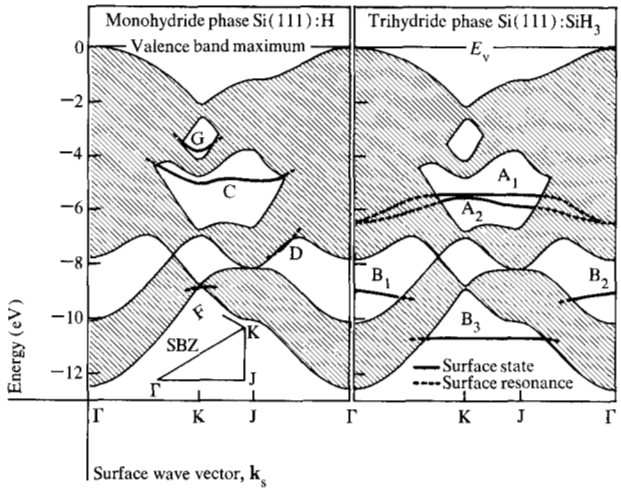

Figure 4 Surface state energy bands of the hydrogen-saturated monohydride (left panel) and trihydride (right panel) phases. Notations for the symmetry points in the surface Brillouin zone (SBZ), the irreducible part of which is also shown, are the same as in [5] (i.e., zone center, edge center, and corner are denoted by Γ, J, and **K**, respectively).

calculations as a function of the slab thickness [12]. Only the local density of states at the second Si layer shows any significant structure due to surface states.

The surface state energy bands giving rise to the structures in the local densities of states are shown in Fig. 4. These bands are plotted along the symmetry directions in the two-dimensional surface Brillouin zone (SBZ) [6]. In the energy regions shown by the cross-hatched area, bulk states are available, so that no truly localized surface states can exist, except for symmetry reasons. However, even in these regions, surface resonances that can give large contributions to local densities of states can occur. True surface states are shown in Fig. 4 by solid lines; resonances are shown by dashed lines. Note that along the Γ-J line, true surface states exist in the nonallowed energy regions for symmetry reasons. This situation is similar to the backbonding surface states [6] of the clean relaxed Si(111) surface. Surface state bands giving rise to the peaks A, B, and C in Fig. 2 are marked by the corresponding letters.

In order to make a direct comparison between theory and experiment, a theoretically simulated spectrum [12] was obtained by superposition of the local densities of states for various layers weighted by an exponential escape factor arising from the small escape depth (assumed to be 0.5 nm) of the photoexcited electrons. To take into account the change in oscillator strength at the surface (associated with hydrogen chemisorption), we have used a value of 5 for the r factor [12, 27] for both the monohydride and trihydride phases. The resulting theoretical spectra for the two phases, broadened by a Lorentzian function of half width (0.7 eV) to simulate experimental broadening, are shown in Fig. 5, where they are compared with the corresponding UPS spectra of hydrogen-covered Si(111)1×1 surfaces. Theoretical spectra obtained in this way represent the distribution of primary electrons only. In order to make a better comparison, we have also added the contributions due to secondary electrons [12] in the theoretical spectra of both phases. The energy distributions of secondary electrons are structureless and thus give only a smooth background. Figure 5 clearly shows that the experimental UPS spectrum of the quenched Si(111)1×1 surface at high hydrogen coverages is in good agreement with the theoretical spectrum for the trihydride phase. The large peaks labeled A and B arise from the corresponding peaks in Fig. 3 and are due to electrons in the orbitals of π and σ symmetry, respectively. We also compare the theoretical spectrum for the monohydride phase with the UPS spectrum [3] for the H-saturated Si(111)7×7 surface in Fig. 5. The main peak C in this spectrum is due to the σ bonding state. Again, the theoretical and UPS spectra are in good agreement with each other. We can conclude that on the Si(111)7×7 surface H chemisorbs in the monohydride phase (ignoring the long-range ordering that is responsible for the reconstruction, since it apparently has a rather small effect on the spectrum), while the trihydride phase is formed on the quenched Si(111)1×1 surface at high coverages. As mentioned earlier, the UPS spectra for the H-saturated 7×7 surface and the quenched 1×1 surface at low coverages (intermediate H saturation) are very similar. The only difference is that the peaks in the UPS spectrum of the 1×1 surface are somewhat broader and the valleys are not as deep as in the 7×7 surface. This can easily be explained by assuming that on the quenched surface, both the monohydride and the trihydride phases coexist near intermediate H saturation, the former phase being predominant.

Discussion

In the present semi-empirical tight-binding model for chemisorption, all the Hamiltonian matrix elements between orbitals of the substrate and the chemisorbed atom are derived from experimental data on molecular ionization potentials through least-squares fitting. Such a determination of the interaction parameters is clearly meaningless if the molecular ionization potentials are less sensitive to these parameters than are the surface states and resonances. Further, their values may have some uncertainties because of the fitting procedure through which the interaction parameters are obtained. Such a calculation is not reliable if the surface states depend critically on these parameters. In order to study these points and to gain a better insight into the chemisorption of H on Si, we

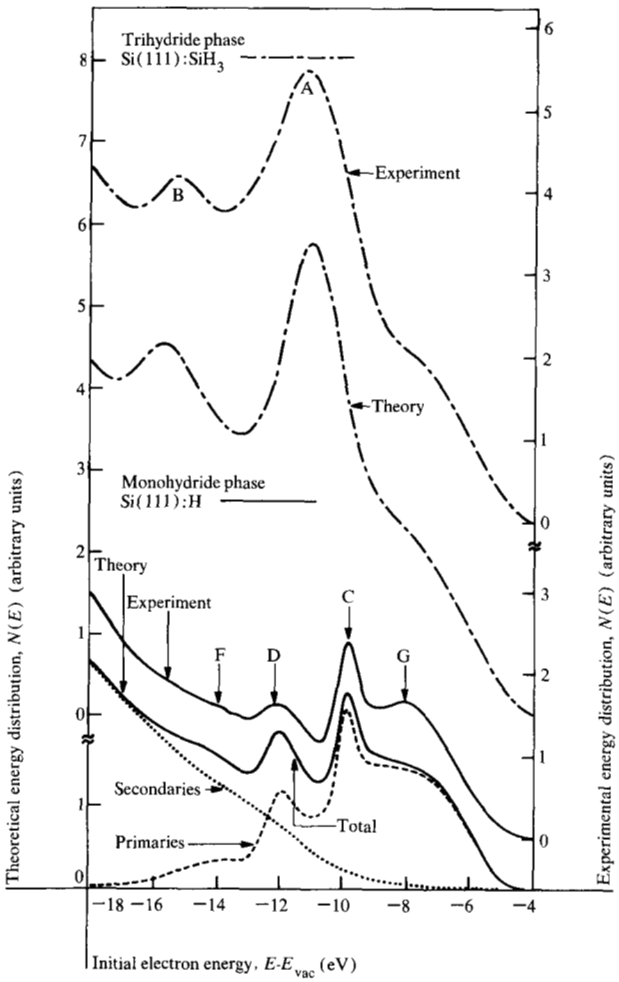

Figure 5 Ultraviolet photoemission spectra of hydrogen-saturated annealed Si(111)7×7 (solid curve, [3]) and hydrogen-saturated quenched Si(111)1×1 (broken curve, [10]) surfaces are compared with the theoretically simulated spectra based on the monohydride and trihydride models for chemisorption, respectively. In the theoretical spectrum for the monohydride phase, separate contributions from primary and secondary electrons are also shown. For clarity, experimental spectra are shifted upward. Photon energy was 21.2 eV.

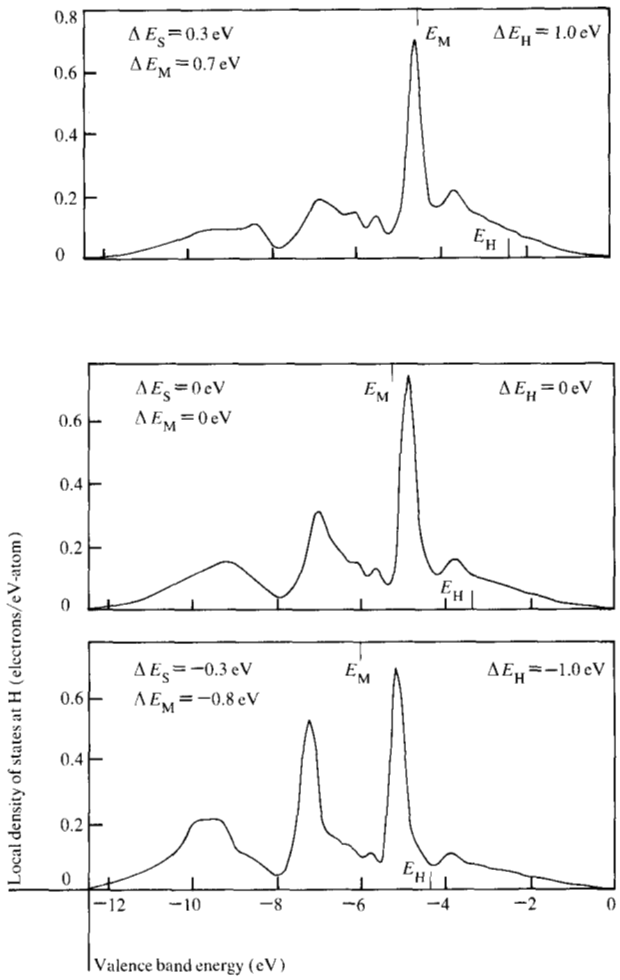

Figure 6 Dependence of the local density of states at the surface hydrogen layer (in the monohydride phase) on the energy E_s(H) of the hydrogen s orbital. Change in the parameter E_s(H) from its fitted value is denoted by ΔE_H. Corresponding changes in the energies of the a_1 molecular orbital of SiH_4 and the hydrogen-induced peak in the local density of states for the monohydride phase are denoted by ΔE_M and ΔE_S, respectively.

have calculated the surface energy bands and local densities of states for various sets of interaction parameters.

We find that the molecular ionization potentials are much more sensitive to changes in the interaction parameters than are the surface states and resonances. The relative insensitivity of the surface states is due mainly to two facts. First, to a large degree, the existence of a surface state depends on the surface geometry and the bulk energy bands of the substrate, since both of these determine the forbidden energy regions (for a given $\mathbf{k}_s$) in which the surface states are pinned [9]. Second, at the surface only one of the Si–H bonds (as opposed to all four in the SiH_4 molecule) is altered as a result of changes in the interaction parameters.

To give one example of the variation of surface state energies with interaction parameters, in Fig. 6 we show the local densities of states at the hydrogen layer (in the monohydride phase) using three sets of parameters obtained by simply changing E_s(H), the s-orbital energy of the hydrogen atom. This is the most important of the parameters because it determines the overall position of the hydrogen-associated peak in the local densities of states near the surface. Since the local density of states can be measured directly in UPS and gives an overall description of surface states, we limit our discussion to it rather than the individual surface state bands. The central panel in Fig. 6 shows the local density of states corresponding to the fitted (i.e., derived from molecular ionization poten-

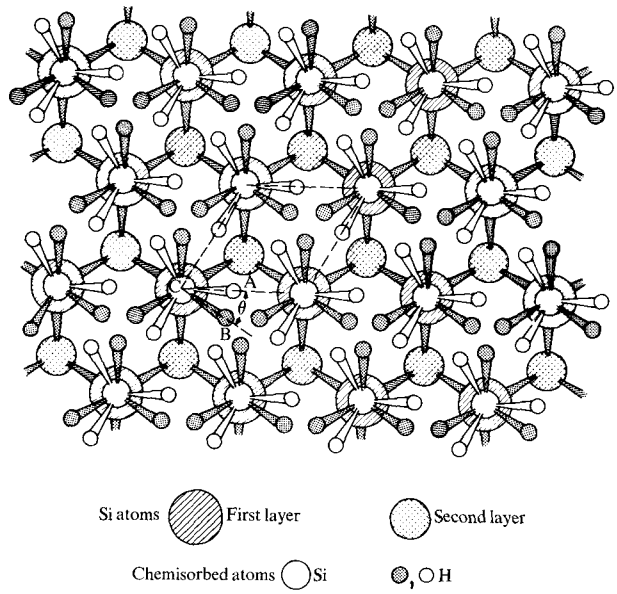

Figure 7 Two of the possible structural models of the trihydride phase Si(111):SiH_3 obtained by changing the relative orientation of the SiH_3 radical and the underlying Si lattice.

Figure 8 Variation of the energy distribution of the simulated theoretical spectrum for the trihydride phase with the H-H interaction parameter V_{HH}. All matrix elements except V_{HH} were kept fixed at their previously determined values.

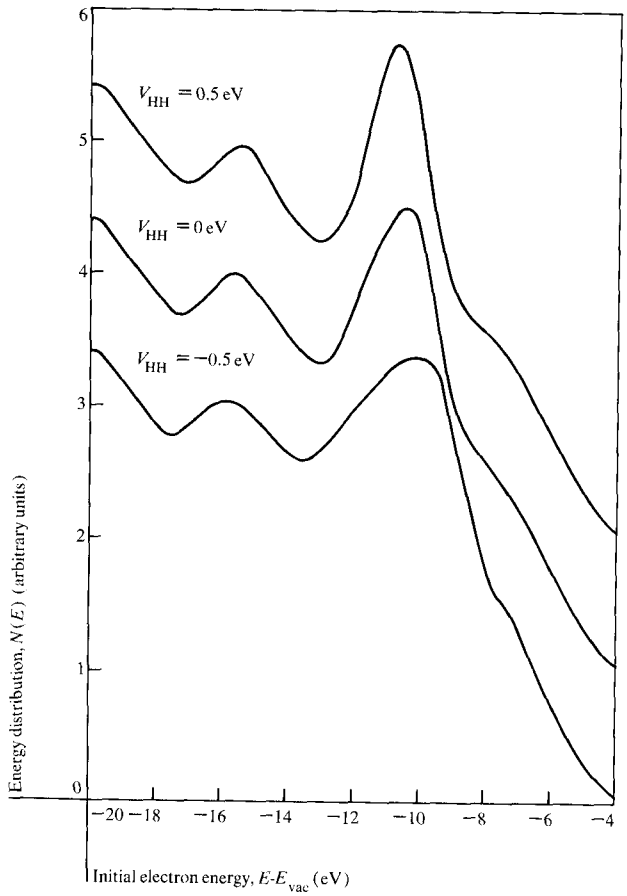

tials) value of E_s(H). This is the same as the upper curve in Fig. 2. The lower and upper panels show the effects of respectively decreasing and increasing the value of E_s(H) by 1.0 eV, while keeping all other parameters fixed at their fitted values (given in Tables 2 and 3). In Fig. 6, the change in the parameter E_s(H) from its fitted value is denoted by ΔE_H. Corresponding changes in the energies of the a_1 molecular orbital of SiH_4 and the hydrogen-induced peak in the local density of states for the monohydride phase are denoted by ΔE_M and ΔE_S, respectively. Any uncertainties in the values of parameters obtained from fitting are likely to be much smaller than 1.0 eV. Rather large changes have been used here simply to produce a noticeable change in the local density of states. As expected, occupied states move nearly rigidly with changes in E_s(H). However, the most important point to notice in Fig. 6 is that none of the qualitative features (number of peaks, their relative heights, widths, etc.) is altered. Compared to the changes in the molecular ionization potentials, even quantitative changes are small. We have also studied the effect of other parameters and, in all cases, we find that the local density of states is relatively insensitive (compared with the molecular orbital energies of SiH_4) to small changes in these parameters. In particular, none of the qualitative features is affected by such changes. We conclude that small uncertainties in the values of parameters are not significant and their determination by fitting to the molecular data is justified.

One of the major uncertainties in our proposed structural model for the trihydride phase is the orientation of the SiH_3 radical relative to the underlying crystal. Two of the possible structures are shown in Fig. 7. The structure shown by filled circles is the normal staggered structure similar to Si_2H_6. The other structure is derived by rotating each SiH_3 radical by 30° about the Si–Si bond. These two structures are characterized by the smallest and largest second-neighbor H-H separation. In principle, all other structures differing in this rotation angle are also possible. However, if there is any interaction between the hydrogen atoms belonging to different SiH_3 radicals, one of the structures shown in Fig. 7 will be favored over all others on energy considerations. From our previous discussions, it seems likely that because of some charge transfer the hydrogen atoms would repel each other and would prefer the configuration shown by open circles. In the results presented for the trihydride phase, this particular configuration was used. However, the results are insensitive to changes in configuration alone, if the second-neighbor H-H interactions are ignored. For the determination of the orientation of SiH_3 radicals, second-neighbor interactions must be included. In Fig. 8, we show theoretical spectra for the trihydride phase, using three different values (−0.5, 0.0, and 0.5 eV) for the H-H interaction parameter V_{HH}. None of the qualitative fea-

tures of the spectra is affected even by large changes in V_{HH}. The only noticeable effect is a broadening of the main surface state peak as the interaction becomes increasingly attractive. Though the effects are small, it seems that a repulsive interaction is better able to explain the UPS data, so that the configuration shown by open circles is more probable.

Acknowledgments

This work was supported in part by the U.S. Air Force Office of Scientific Research (AFSC), under contract F44620-76-C0041. The author is grateful to D. E. Eastman for stimulating discussions and valuable comments on the manuscript.

References and notes

1. D. E. Eastman and W. D. Grobman, *Phys. Rev. Lett.* **28,** 1378 (1972); L. F. Wagner and W. E. Spicer, *Phys. Rev. Lett.* **28,** 1381 (1972).
2. J. E. Rowe and H. Ibach, *Phys. Rev. Lett.* **32,** 421 (1974).
3. T. Sakurai and H. D. Hagstrum, *Phys. Rev. B* **12,** 5349 (1975).
4. For a recent review of the theoretical studies of semiconductor surface states, see for example J. A. Appelbaum and D. R. Hamann, *Rev. Mod. Phys.* **48,** 479 (1976).
5. K. C. Pandey and J. C. Phillips, *Phys. Rev. Lett.* **32,** 1433 (1974); K. C. Pandey and J. C. Phillips, *Solid State Commun.* **14,** 439 (1974).
6. K. C. Pandey and J. C. Phillips, *Phys. Rev. B* **13,** 750 (1976).
7. K. C. Pandey and J. C. Phillips, *Phys. Rev. Lett.* **34,** 1450 (1975).
8. J. J. Lander and J. Morrison, *J. Chem. Phys.* **37,** 729 (1962).
9. J. E. Rowe and J. C. Phillips, *Phys. Rev. Lett.* **32,** 1315 (1974).
10. K. C. Pandey, T. Sakurai, and H. D. Hagstrum, *Phys. Rev. Lett.* **35,** 1728 (1975).
11. In addition to the quenched 1×1 surface, there are a number of other 1×1 surfaces that are stabilized by small amounts ($\approx$0.05 monolayer) of various impurities such as Te, Cl, etc. Apart from the presence of impurities, it is not clear whether the quenched and impurity-stabilized surfaces have the same surface atomic arrangements. For a discussion of the impurity-stabilized 1×1 surfaces, see for example H. D. Shih, F. Jona, D. W. Jepsen, and P. M. Marcus, *Phys. Rev. Lett.* **37,** 1622 (1976) and J. V. Florio and W. D. Robertson, *Surface Sci.* **24,** 173 (1971).
12. K. C. Pandey, *Phys. Rev. B* **14,** 1557 (1976).
13. H. Ibach and J. E. Rowe, *Surface Sci.* **43,** 481 (1974).
14. Traditionally, LEED has been used for the structural determination of ordered solid surfaces. (For a general discussion of LEED, see for example J. B. Pendry, *Low Energy Electron Diffraction*, Academic Press, Inc., London, 1974.) However, because of the multiple scattering, a dynamic LEED analysis is very difficult and time consuming. Consequently, only in simple cases (especially metal surfaces) where the surface unit cell is small and surface atoms are perturbed only slightly from their ideal positions, has such an approach been applied with any success. Because of the relatively weak scattering of electrons from H atoms, the LEED spectra are insensitive to these atoms and their positions cannot be determined from LEED. This is a serious limitation of the LEED method. For the present system [H on Si(111)] no quantitative measurements of LEED spectra have been made.
15. L. Pauling, *The Nature of the Chemical Bond*, third ed., Cornell University Press, Ithaca, NY, 1960.
16. L. E. Sutton, ed., *Tables of Interatomic Distances and Configurations in Molecules and Ions*, The Chemical Society, London, 1958.
17. J. A. Appelbaum and D. R. Hamann, *Phys. Rev. Lett.* **34,** 806 (1975).
18. J. A. Pople and D. L. Beveridge, *Approximate Molecular Orbital Theory*, McGraw-Hill, Inc., New York, 1970.
19. J. C. Slater and G. F. Koster, *Phys. Rev.* **94,** 1498 (1954).
20. T. Koopmans, *Physica* **1,** 104 (1933).
21. W. G. Richards, *Intl. J. Mass. Spectrom. & Ion Phys.* **2,** 419 (1969).
22. R. G. Cavell, S. P. Kowalczyk, L. Ley, R. A. Pollack, B. Mills, D. A. Shirley, and W. Perry, *Phys. Rev. B* **7,** 5313 (1973).
23. A. W. Potts and W. C. Price, *Proc. Roy. Soc. A* **326,** 165 (1972); W. C. Price and G. R. Wilkinson, unpublished results.
24. M. L. Sink and G. E. Juras, *Chem. Phys. Lett.* **20,** 474 (1973).
25. The assignment of the symmetry orbitals to the various ionization potentials of the molecules was made on the basis of the vibrational fine structures of the photoemission spectra, the relative strengths of various peaks, and in some cases by using elaborate molecular orbital calculations. A discussion of these assignments can be found in [22–24].
26. K. Hirabayashi, *J. Phys. Soc. Jpn.* **27,** 1475 (1969).
27. K. C. Pandey and J. C. Phillips, *Solid State Commun.* **19,** 69 (1976).

Received October 25, 1977; revised December 20, 1977

The author is located at the IBM Thomas J. Watson Research Center, Yorktown Heights, New York 10598.